Published in final edited form as:
*Neuroimage*. 2009 April 1; 45(2): 477–489. doi:10.1016/j.neuroimage.2008.12.003.

# Differential visually-induced gamma-oscillations in human cerebral cortex

**Eishi Asano**[1,2,*], **Masaaki Nishida**[1], **Miho Fukuda**[1], **Robert Rothermel**[3], **Csaba Juhasz**[1,2], and **Sandeep Sood**[4]

[1] Department of Pediatrics, Children's Hospital of Michigan, Detroit, Michigan, 48201, USA

[2] Department of Neurology, Children's Hospital of Michigan, Detroit, Michigan, 48201, USA

[3] Department of Psychiatry, Children's Hospital of Michigan, Detroit, Michigan, 48201, USA

[4] Department of Neurosurgery, Children's Hospital of Michigan, Detroit, Michigan, 48201, USA

## SUMMARY

Using intracranial electrocorticography, we determined how cortical gamma-oscillations (50–150Hz) were induced by different visual tasks in nine children with focal epilepsy. In all children, full-field stroboscopic flash-stimuli induced gamma-augmentation in the anterior-medial occipital cortex (starting on average at 31-msec after stimulus presentation) and subsequently in the lateral-polar occipital cortex; minimal gamma-augmentation was noted in the inferior occipital-temporal cortex; occipital gamma-augmentation was followed by gamma-attenuation in three children. Central-field picture-stimuli induced sustained gamma-augmentation in the lateral-polar occipital cortex (starting on average at 69-msec) and subsequently in the inferior occipital-temporal cortex in all children and in the posterior frontal cortex in three children; the anterior-medial occipital cortex showed no gamma-augmentation but rather gamma-attenuation. Electrical stimulation of the anterior-medial occipital cortex induced a phosphene in the peripheral-field or eye deviation to the contralateral side, whereas that of the lateral-polar occipital cortex induced a phosphene in the central-field. In summary, full-field, simple and short-lasting visual information might be preferentially processed by the anterior-medial occipital cortex, and subsequently by the lateral-polar occipital cortex. Gamma-attenuation following augmentation in the striate cortex might be associated with a relative refractory-period to flash-stimuli or feed-forward inhibition by other areas. Central-field complex visual information might be processed by a network involving the lateral-polar occipital cortex and the inferior occipital-temporal cortex. A plausible interpretation of posterior-frontal gamma-augmentation during central-field picture stimuli includes activation of the frontal-eye-field for visual searching. Gamma-attenuation in the anterior-medial occipital cortex during central-field picture-stimuli might be associated with relative inattention to the peripheral visual field during central-field object visualization.

## INTRODUCTION

Previous studies using neuroimaging and neurophysiologic techniques have increased our understanding in the functional architecture of the human visual system, but the short-latency

*Corresponding Author: Eishi Asano, MD, PhD, MS (CRDSA), Address: Division of Pediatric Neurology, Children's Hospital of Michigan.,3901 Beaubien St., Detroit, MI, 48201, USA. Phone: 313-745-5547; FAX: 313-745-0955; E-mail: eishi@pet.wayne.edu.

dynamics of visual processing involving both anterior-medial and lateral polar occipital cortices have not been fully elucidated. Neuroimaging techniques such as functional MRI (Levy et al., 2001; Prado et al., 2005; Stenbacka and Vanni, 2007; Di Russo et al., 2007; Yotsumoto et al., 2008) and positron emission tomography (Nobre et al., 1997; Vandenberghe et al., 2000) have good spatial but insufficient temporal resolution to assess such short-latency cortical dynamics. Noninvasive neurophysiologic techniques such as event-related potentials (ERPs) on scalp EEG (Tallon-Baudry et al., 1996; Csibra et al., 2000; Ohla et al., 2007) and event-related magnetic fields on magnetoencephalography (MEG) (Pavlova et al., 2004; Inui et al., 2006; Poghosyan and Ioannides, 2007) have good temporal resolution to assess such cortical dynamics involving the lateral cortices, but poor signal-noise ratio in measurement of cortical activity from deeply-situated cortices such as anterior-medial occipital and inferior occipital-temporal cortices. It has been reported that scalp EEG recording may provide inaccurate estimation of the deep source (Wang and Gotman, 2001). Intracranial electrocorticography (ECoG) recording using subdural electrodes in presurgical evaluation for patients with uncontrolled epilepsy can offer a unique situation to study the short-latency dynamics of cortical processing involving the deeply-situated cortices with a spatial resolution of 1 cm or below and a temporal resolution of 10 msec or below (Bruns and Eckhorn., 2004; Huettel et al., 2004; Lachaux et al., 2005; Tallon-Baudry et al., 2005; Gaillard et al., 2006; Farrell et al., 2007; Yoshor et al., 2007).

Previous human studies of event-related spectral analysis of intracranial ECoG have suggested that augmentation of gamma-oscillations can be used as an electrophysiological marker of local neuronal activation (Crone et al., 1998; Lachaux et al., 2005; Sinai et al., 2005; Tallon-Baudry et al., 2005; Miller et al., 2007; Privman et al., 2007; Sederberg et al., 2007; Rudrauf et al., 2008). Cortical modulation of gamma-range oscillations associated with visual object processing was demonstrated in both human and animal studies using intracranial ECoG recording (Gray and McCormick, 1996; Kruse and Eckhorn, 1996; Bruns and Eckhorn, 2004; Lachaux et al., 2005; Tallon-Baudry et al., 2005; Tanji et al., 2005; Niessing et al., 2005; Womelsdorf et al., 2006; Privman et al., 2007). Yet due to the limited spatial sampling, the short-latency dynamics of visual processing involving (i) the anterior-medial occipital region, (ii) the lateral-polar occipital region, and (iii) the inferior occipital-temporal region have not been fully elucidated previously.

In the present study of children with focal epilepsy, we specifically hypothesized that full-field stroboscopic flash-stimuli would induce augmentation of gamma-oscillations in the anterior-medial occipital cortex, according to the results of a recent study of six healthy adults using MEG (Inui et al., 2006). We also hypothesized that central-field picture-stimuli would induce augmentation of gamma-oscillations in the lateral-polar occipital cortex and subsequently in the inferior occipital-temporal cortex, according to the results of a previous fMRI study (Levy., 2001). To test these hypotheses, we delineated the dynamic change of cortical gamma-oscillations induced by visual stimuli on an individual three-dimensional MR image. We also determined whether different visual tasks induced differential cortical activations in large cortical networks. We finally determined the spatial relationship between the neural sources of induced gamma-oscillations and the observation of electrical brain stimulation, in order to clarify the functional correlate of modulation of gamma-oscillations on ECoG. In the present study, ‘induced oscillations’ were defined as oscillatory responses consisting of both phase-locked (i.e.: a component present after averaging) and non-phase-locked (a component absent after averaging) components, as defined in a previous study (Fukuda et al., 2008).

# METHODS

## Patients

The inclusion criteria of the present study consisted of: (i) age of two years or above, (ii) normal or corrected-to-normal vision, (iii) a two-stage epilepsy surgery using chronic subdural ECoG recording in Children's Hospital of Michigan, Detroit between October 2006 and September 2007, (iv) functional cortical mapping for the visual area by measurement of visually-induced gamma-oscillations, (v) functional cortical mapping for the visual area using electrical stimulation, (vi) subdural electrode placement involving the anterior-medial occipital region (defined as the anterior-medial surface of Brodmann Area 17/18 in the present study), (vii) subdural electrode placement involving the lateral-polar occipital region (defined as the lateral-to-polar surface of Brodmann Area 17/18), and (viii) subdural electrode placement involving the inferior occipital-temporal region (defined as the inferior surface of Brodmann Area 19/37) (Talairach and Tournoux, 1988). The exclusion criteria consisted of: (i) a visual-field deficit detected by confrontation tests prior to surgery, (ii) the presence of MRI-visible structural lesion involving the occipital cortex, (iii) the presence of massive brain malformations (such as large porencephaly or perisylvian polymicrogyria) which are known to confound the anatomical landmarks for the central sulcus or calcarine sulcus, (iv) history of previous brain surgery, and (v) history of photosensitivity or photo-paroxysmal response on previous scalp EEG recordings. We studied a consecutive series of nine children (age: 3 years - 17 years; five girls and four boys) who satisfied the inclusion and exclusion criteria (Table 1). Seven children were right-handed, and the remaining two children with the epileptogenic focus localized in the left hemisphere were left-handed (Table 1). The study has been approved by the Institutional Review Board at Wayne State University, and written informed consent was obtained from the parents or guardians of all subjects.

## Subdural electrode placement

For extraoperative video-ECoG recording, platinum grid electrodes (10mm inter-contact distance; 4mm diameter; Ad-tech, Racine, WI, USA) were surgically implanted on the presumed epileptogenic hemisphere (right-sided implantation in six children and left-sided implantation in three). As shown in our previous report (Fukuda et al., 2008), all electrode plates were stitched to adjacent plates and/or the edge of the dura mater to avoid movement. In addition, intraoperative photographs were obtained with a digital camera before dural closure to enhance the spatial accuracy of electrode display on the three-dimensional brain surface reconstructed from MRI. Placement of intracranial electrodes was guided by the results of scalp video-EEG recording, structural lesions on MRI, and glucose-metabolism positron emission tomography. Subdural strip electrodes were placed in the posterior head region, in order to determine the posterior resection margin. The lateral portion of pre- and post-central gyri was also covered with electrodes for subsequent functional mapping in all nine cases. The total number of electrode contacts ranged from 96 to 128 for each patient.

## Coregistration of subdural electrodes on individual three-dimensional MRI

MRI including a T1-weighted spoiled gradient echo image as well as fluid-attenuated inversion recovery image was obtained preoperatively. Planar x-ray images (lateral and anteroposterior) were acquired with the subdural electrodes in place for electrode localization on the brain surface; three metallic fiducial markers were placed at anatomically well-defined locations on the patient's head for co-registration of the x-ray image with the MRI (von Stockhausen et al., 1997; Muzik et al., 2007). A three-dimensional surface image was created with the location of electrodes as directly defined on the brain surface, as previously described (von Stockhausen et al., 1997; Muzik et al., 2007; Brown et al., 2008; Fukuda et al., 2008). The accuracy of this procedure was reported previously as 1.24 ± 0.66 mm with a maximal misregistration of 2.7 mm (von Stockhausen et al., 1997).

### Extraoperative video-ECoG recording

Extraoperative video-ECoG recordings were obtained for three to five days, using a 192-channel Nihon Kohden Neurofax 1100A Digital System (Nihon Kohden America Inc, Foothill Ranch, CA, USA), which has an input impedance of 200 MΩ, a common mode rejection ratio greater than 110 dB, an A/D conversion of 16 bits, a sampling frequency at 1,000-Hz and the amplifier band pass at 0.08- to 300-Hz. The averaged voltage of ECoG signals derived from the fifth and sixth electrodes (system reference potential) was used as the original reference. ECoG signals were then re-montaged to a common average reference, as previously reported (Crone et al., 2001). Channels contaminated with large interictal epileptiform discharges or artifacts were excluded from the common average reference (Fukuda et al, 2008). No notch filter was used for further analysis in any subjects (Brown et al., 2008; Fukuda et al., 2008). As a part of clinical procedures, surface electromyography electrodes were placed on the left and right deltoid muscles, and electrooculography electrodes were placed 2.5 cm below and 2.5 cm lateral to the left and right outer canthi. Antiepileptic medications were discontinued or reduced during ECoG monitoring until a sufficient number of habitual seizures were captured, and seizure onset zones were identified as described in our previous reports (Brown et al., 2008; Fukuda et al., 2008).

### Visual tasks

**Full-field stroboscopic flash stimuli—**All tests necessary for visual mapping by measurement of visually-induced gamma-oscillations were performed while each patient was awake, unsedated, and comfortably seated on the bed in a room with all lights off (Tanji et al., 2005). Yet, complete darkness in the room (Vingerhoets et al., 2007) was not tenable in the present study, since each patient was connected to several bio-monitoring systems placed outside the patient's visual field. During video-ECoG recording, a series of 20 full-field stroboscopic flash stimuli were given to each patient with a frequency of 1 Hz, at a distance of 30 cm from the closed eyes (Coburn et al., 2005), using the square-shape xenon photic stimulator LS-703A (Nihon Kohden America Inc), which is connected to the Digital EEG system via the TTL trigger signal, has a stimulus field size of 13 × 3.5 cm, a maximum flash energy of 1.28 J, a flash duration of 20 μsec, and a mean luminance of 30,000 cd/$m^2$.

**Central-field picture stimuli—**During video-ECoG recording, a series of 60 central-field picture stimuli were presented to each patient, using a 17-inch Acer AL1714 LCD computer monitor (Acer America, San Jose, CA, USA) placed 60 cm in front of subjects; the monitor cables and power cables were placed at least 60cm away from the subject as well as the ECoG Recording System. The monitor had a refresh rate of 75 Hz and a luminance of 370 cd/$m^2$. Picture stimuli consisted of 20 faces, 20 houses and 20 abstract shapes (Woods et al., 2004), of which size ranged from 6–10 cm in height and width. Picture stimuli were binocularly presented at the center of the monitor, in grayscale, on the black background, in a pseudorandom order, for 1,000 msec with an inter-stimulus interval of 1,000 msec, using Presentation Software (Neurobehavioral Systems Inc, Albany, CA, USA). A trigger signal synchronized with the onset of each picture presentation was delivered to the ECoG recording system by a Windows-98 PC computer running the Presentation Software.

### Time-frequency analysis of ECoG time-locked to the onset of visual stimulus

Event-related amplitude modulations were evaluated using the trigger point set at the onset of visual stimulus. ECoG data were analyzed using BESA® EEG V.5.1.8 software (Hoechstetter et al., 2004; MEGIS Software GmbH, Gräfelfing, Germany), and the following time-frequency ECoG analysis was employed to a series of ECoG epochs time-locked with the onset of visual stimulus. The length of each ECoG epoch (trial) was 1,000 msec (starting 250-msec before

and ending 750-msec after the trigger) for the analysis of ECoG modulation induced by full-field stroboscopic flash stimulus.

The length of ECoG epoch was 2,000 msec (starting 500-msec before and ending 1,500-msec after the trigger) for the analysis of ECoG modulation induced by central-field picture stimulus. The inclusion criteria defining ECoG epochs suitable for this time-frequency analysis for full-field flash stimuli included: the subject faced towards the photic stimulator without blockage by hand or arm. The inclusion criteria for central-field picture stimuli included: the subject apparently watched the monitor with the eyes opened according to the simultaneous video recording. The exclusion criteria included: i) visual assessment revealed that ECoG trace was affected by movement artifacts (Klem, 2003); ii) visual ECoG assessment revealed that interictal epileptiform discharges were present at an occipital channel; iii) ECoG trace was affected by electrographic seizures. In order for data analysis to progress to completion, at least 50% of ECoG epochs must have satisfied the above criteria. If a child failed to have 50% of ECoG epochs satisfying the above criteria, a repeat task was employed in the following day. All ECoG epochs which satisfied all of the inclusion and exclusion criteria were utilized for the time-frequency ECoG analysis described below.

Each suitable ECoG epoch was transformed into the time-frequency domain using complex demodulation technique as featured in the BESA software (Hoechstetter et al., 2004; Fan et al., 2007; Brown et al., 2008; Fukuda et al., 2008). In that technique, the time-frequency transform was obtained by multiplication of the time-domain signal with a complex exponential, followed by a low pass finite impulse response (FIR) filter of Gaussian shape. Details on the complex demodulation technique for time-frequency transformation are described elsewhere (Papp and Ktonas, 1977; Hoechstetter et al., 2004). This is equivalent to a wavelet transformation with constant wavelet width across frequencies. As a result of this transformation, the signal was assigned a specific amplitude and phase as a function of frequency and time (relative to the onset of visual stimulus). In the present study, only the amplitude (i.e.: square root of power) averaged across all trials, was used for further analysis. It was previously reported that the amplitude spectrum is easier to visually relate to the raw signal record than is the power spectrum (da Silva, 1999). Time-frequency transformation was performed for gamma-band frequencies between 30- and 200-Hz and latencies between 250-msec before and 750-msec after the trigger for the analysis of ECoG modulation induced by full-field stroboscopic stimulus, in steps of 5-Hz and 10-msec as performed in our previous study (Brown et al., 2008). This corresponded to a time-frequency resolution of +/−7.1 Hz and +/−15.8 msec (50% power drop of the FIR filter). We recognize that this time-frequency resolution is suited to the analysis of short-latency visually-induced gamma-oscillations but may not be suited to analyze slower and narrow-frequency oscillations such as alpha-band oscillations. Similarly, time-frequency transformation was performed for the same gamma-band frequencies and latencies between 500-msec before and 1,500-msec after the trigger for the analysis of ECoG modulation induced by central-field picture stimulus.

At each time-frequency bin (with a size of 5-Hz and 10-msec), we analyzed the percentage change in amplitude (averaged across trials) relative to the mean amplitude in a reference period, defined as the resting state prior to visual stimuli. This parameter is commonly termed “event-related synchronization and desynchronization” (Pfurtscheller, 1977), whereas a less suggestive terminology is “temporal spectral evolution” (TSE) (Salmelin and Hari, 1997). In the present study, the reference period for full-field stroboscopic flash stimulus was set at a period of 250 msec immediately prior to the onset of visual stimulus. The reference period for central-field picture stimulus was set at a period of 500 msec immediately prior to the onset of visual stimulus. We assumed that the above reference periods consisted of the baseline resting state in the present study.

To test for statistical significance for each obtained TSE value, two-step statistics was performed using the BESA software: First, statistics based on bootstrapping approach (Davidson et al., 1999) was applied to obtain an uncorrected p-value at each time-frequency bin. In a second step, correction for multiple testing was performed, since each electrode was analyzed at 3,500 time-frequency bins per 1,000 msec, with TSE values at neighboring bins being partially dependent. A modification of the correction developed by Simes (1986) was used as suggested for time-frequency analysis by Auranen (2002): p values of one frequency bin and channel were sorted in ascending order ($p_i$, i=1, …, N). The maximum index m in the sorted array for which $p_i < \alpha*i/N$ was determined. All uncorrected p-values with i<m were accepted as significant. The corrected significance level α was set to 0.05. This approach is less conservative than the classic Bonferroni correction and is specifically suited for partially dependent multiple testing (Simes, 1986; Auranen, 2002). In all figures in the present study, red color indicated a significant increase of amplitude, blue color a significant decrease in the corresponding time-frequency bin relative to the baseline during the reference period.

Since the number of subdural electrodes ranged from 96 to 128 across subjects, an additional correction for testing in multiple electrodes was employed, as described in our previous study (Brown et al., 2008). TSE values in a given electrode were declared to be statistically significant only if a minimum of 8 voxels in the gamma-band range were arranged in a continuous array spanning (i) at least 20-Hz in width and (ii) at least 20-msec in duration. Such correction provides a very small probability of Type-I error in determination of gamma-augmentation or attenuation. We recognize that this analysis may potentially underestimate gamma-modulations with a restricted frequency band (less than 20-Hz in width) or that with a short duration (less than 20-msec in duration). The onset latency of induced gamma-augmentation was defined as the initial epoch showing a significant gamma-augmentation according to the above-mentioned criteria (Brown et al., 2008).

### Visual mapping using neurostimulation

Visual mapping by neurostimulation was performed during extraoperative ECoG recording, using a method similar to those described previously (Farrell et al., 2007; Miller et al., 2007; Brown et al., 2008; Fukuda et al., 2008). A pulse-train of electrical stimuli was delivered using the Grass S88 constant-current stimulator (Astro-Med, Inc, West Warwick, RI, USA); clinical responses associated with stimulations were observed by at least two investigators. In order to minimize the risk of a subject feeling scared or overwhelmed, each subject was informed that she/he might have a temporary sensorimotor, auditory, visual or language symptom, prior to the initiation of neurostimulation study. Each subject was aware of the timing of each stimulation trial but unaware of the location of stimulated sites. To minimize the risk of stimulation-induced seizures, a loading dose of phenytoin (20 mg/kg) was administered intravenously prior to the mapping session (Fukuda et al., 2008). To determine the presence of after-discharges, video-ECoG was recorded continuously during the procedure.

Subdural electrode pairs were stimulated by an electrical pulse-train of 10-sec maximum duration using pulses of 300 μsec duration. Initially, stimulus intensity was set to 3-mA and stimulus frequency was set to 50 Hz. Stimulus intensity was increased from 3- to 9-mA in a stepwise manner by 3-mA until a clinical response or after-discharge was observed. When after-discharge threshold was determined, stimulus intensity above that threshold was not used. When the patient noticed visual symptoms, he/she was asked to tell what he/she noticed and to point out the direction of symptoms. Brain regions at which stimulation consistently induced a clinical response (at least twice in a row) were declared ‘eloquent for that function’. When after-discharge without an observed clinical response or when neither clinical response nor after-discharge was induced by the maximally-intense stimuli, the brain region was declared ‘not proven eloquent’. When both clinical response and after-discharges occurred, another

pulse-train of the same or 1-mA smaller intensity was used until either clinical response or after-discharge failed to develop.

### Delineation of ECoG data on three-dimensional MRI

ECoG data for each electrode channel were exported to the given electrode site on the individual three-dimensional brain surface in two different ways (Figures 1–3). In order to delineate *'when', 'where'* and *'at what frequency band'* significant alteration of spectral amplitude occurred, time-frequency plot matrixes created above were placed onto a three-dimensional MRI at the cortical sites corresponding to their respective subdural electrode positions. In order to animate *'when', 'where'* and *'how many fold'* gamma-oscillations were increased or decreased, 'gamma-range amplitude' (defined as the spectral amplitude averaged across 50- to 150-Hz frequency bands and normalized to that of the reference period) was sequentially delineated on the individual three-dimensional MRI (Figures 1 and 2; Videos S1–S4), using a method previously described (Brown et al., 2008). 'Gamma-range amplitude' was calculated without a frequency band at 60Hz if visual inspection revealed a 60-Hz artifact peak on the amplitude spectral curve for all subdural electrodes (Nishida et al, 2007). 'Gamma-range amplitude' for each electrode channel at each 10-msec epoch was registered into the SurGe Interpolation Software 1.2 (Web site: http://mujweb.cz/www/SurGe/surgemain.htm), and interpolated topography map of 'gamma-range amplitude' at each 10-msec epoch was accurately superimposed to the individual three-dimensional MRI. This procedure yielded a movie file showing a sequential alteration of gamma-oscillations induced by visual stimuli (Brown et al., 2008).

## RESULTS

### Visual assessment of ECoG traces during visual tasks

Full-field flash stimuli were satisfactorily given to all subjects; none of the ECoG epochs were affected by movement artifacts, interictal epileptiform discharges involving the occipital sites or electrographic seizures. Thus, all epochs were included into the analysis of ECoG modulation induced by full-field flash stimuli.

During the presentation of central-field picture stimuli, on the other hand, a 5-year-old girl (patient #3) had interictal spike-wave bursts at 1–4 Hz intermittently involving the occipital electrodes; visual assessment revealed that interictal epileptiform discharges were present in the occipital sites in 32 of the 60 ECoG epochs (53%) (Figure 4). Thus, a repeat session of central-field picture presentation was employed to this subject in the following day, when interictal spike-wave discharge was absent at occipital sites; all ECoG epochs in the second session were utilized for further analysis of patient #3. The remaining eight subjects did not have ECoG epochs affected by movement artifacts, interictal epileptiform discharges involving the occipital sites or electrographic seizures; thus, all epochs were included into the analysis of ECoG modulation induced by central-field picture stimuli.

### Spectral amplitude modulations associated with full-field stroboscopic flash stimuli

Spatial and temporal patterns of amplitude modulations associated with full-field stroboscopic flash stimuli are summarized in Table 2. Full-field stroboscopic flash stimuli resulted in visually-induced gamma oscillations (most prominent at 50–150 Hz range) initially augmented in the anterior-medial occipital region (the anterior-medial surface of Brodmann Area 17/18) in all nine children; such anterior-medial occipital gamma augmentation became significant, on average, at 31 msec after stimulus presentation (standard deviation [SD]: 7.8 msec; 95% confidence interval [95%CI]: 25 to 37 msec). The mean offset latency of such anterior-medial occipital gamma augmentation was 187 msec (SD: 78 msec; 95%CI: 116 to 237 msec). The mean duration of such anterior-medial occipital gamma augmentation was 156 msec (SD: 80

msec; 95%CI: 94 to 217 msec). The maximal increase of 'gamma-range amplitude' in the anterior-medial occipital region was 202% on average across nine patients (SD: 116%). In three children (patients #3, 5, and 7), visually-induced gamma augmentation in the anterior-medial occipital region was subsequently followed by temporary gamma attenuation (compared to the baseline measures) in the same or adjacent electrodes (Table 2).

Significant gamma-augmentation involving the lateral-polar occipital region (the lateral-to-polar surface of Brodmann Area 17/18) was noted in seven children. In five subjects (patients #4, 5, 7, 8 and 9; Table 2), such lateral-polar occipital gamma augmentation became significant 20–30 msec after anterior-medial occipital gamma augmentation became significant. In two subjects (patients #2 and 6; Table 2), both lateral-polar and anterior-medial occipital gamma augmentation simultaneously became significant. The mean onset latency of flash-induced gamma augmentation in the lateral-polar occipital region was 44 msec (SD: 9.8 msec; 95%CI: 35 to 53 msec). The mean offset latency of flash-induced gamma augmentation in the lateral-polar occipital region was 160 msec (SD: 51 msec; 95%CI: 113 to 207 msec). The mean duration of flash-induced gamma augmentation in the lateral-polar occipital region was 126 msec in these seven subjects (SD: 50 msec; 95%CI: 79 to 172 msec). The maximal increase of 'gamma-range amplitude' in the lateral-polar occipital region was 98% on average across seven patients (SD: 50%).

The Wilcoxon Signed Ranks Test suggested that the onset latency of flash-induced gamma augmentation was smaller in the anterior-medial occipital region compared to the lateral-polar occipital region ($p=0.03$) but failed to demonstrate a significant difference in the offset latency between the anterior-medial and lateral-polar occipital regions ($p=0.9$). The Wilcoxon Signed Ranks Test also suggested that the maximal increase of 'gamma-range amplitude' was larger in the anterior-medial occipital region compared to the lateral-polar occipital region ($p=0.04$).

In three children (patients #3, 5, and 7), visually-induced gamma augmentation in the lateral-polar occipital region was subsequently followed by brief gamma attenuation in the same or adjacent electrodes (Table 2; Figure 3). In five children (patients #1, 4, 6, 8 and 9), visually-induced gamma augmentation subsequently involved the inferior occipital-temporal area (the inferior surface of Brodmann Area 19/37); the mean duration of such inferior occipital-temporal gamma augmentation was 142 msec (SD: 82 msec).

### Spectral amplitude modulations associated with central-field picture stimuli

Spatial and temporal patterns of amplitude modulations associated with central-field picture stimuli are summarized in Table 3. Central-field picture stimuli resulted in gamma augmentation (most prominent at 50–150 Hz range) initially involving the lateral-polar occipital region (the lateral-to-polar surface of Brodmann Area 17/18) in all nine children, and such lateral-polar occipital gamma augmentation became significant, on average, at 69 msec after stimulus presentation (SD: 21 msec; 95%CI: 52.3 to 85.4 msec) and persisted during the picture presentation. The mean duration of lateral-polar occipital gamma augmentation was 1,147 msec (SD: 127 msec).

Among electrodes in the lateral-polar occipital region (Figures S1), 'a larger distance of electrode site from the occipital pole' was associated with 'a larger onset latency of induced gamma-augmentation' (mean regression slope across nine patients: 55 msec/cm; SD: 40.5 msec/cm; 95%CI: 23.7 to 86.0 msec/cm). This finding suggests that each 1 cm increase in distance from the occipital pole was associated with a 55 msec increase in the onset latency of induced gamma-augmentation among the analyzed lateral-polar occipital sites. Among electrodes in the lateral-polar occipital region, 'a larger distance of electrode site from the occipital pole' was associated with 'a smaller offset latency of induced gamma-augmentation' (mean regression slope across nine patients: −117 msec/cm; SD: 142 msec/cm;

95%CI: −226 to −7.6 msec/cm). This finding suggests that central-field stimulus-induced gamma-augmentation sustained longer at the site close to the occipital pole and subsided sooner at the site distant from the occipital pole and that each 1 cm increase in distance from the occipital pole was associated with a 117 msec decrease in the offset latency of induced gamma-augmentation among the analyzed lateral-polar occipital sites.

Among electrodes in the lateral-polar occipital region, ‘a larger distance of electrode site from the occipital pole’ was associated with ‘a smaller maximum gamma-range amplitude measure’ (mean regression slope across nine patients: −15.3 %/cm; SD: 16.6 %/cm; 95%CI: −28.0 to −2.6 %/cm). This finding suggests that central-field stimulus-induced gamma-augmentation was more intense at the site close to the occipital pole and less intense at the site distant from the occipital pole and that each 1 cm increase in distance from the occipital pole was associated with a 15.3% decrease in the induced gamma-range amplitude among the analyzed lateral-polar occipital sites.

Visually-induced gamma oscillations subsequently involved the inferior occipital-temporal region (the inferior surface of Brodmann Area 19/37) in all nine subjects. The mean latency of the onset of inferior occipital-temporal gamma augmentation was 132 msec (SD: 52 msec; 95%CI: 92.3 to 172.1 msec). The mean duration of such inferior occipital-temporal gamma augmentations was 928 msec (SD: 265 msec).

Significant gamma-augmentation was subsequently noted in the posterior frontal cortices in three children (patients #1, 4 and 8) (Table 3; Figure 2). None of the children showed augmentation of gamma-oscillations in the anterior-medial occipital cortex during central-field picture stimuli; rather, three children (patients #1, 8 and 9) showed brief gamma attenuation in the anterior-medial occipital cortex during stimulus presentation (Table 3).

## Relationship between presumed visual areas suggested by ECoG analyses and those by neurostimulation

The spatial relationship between the visual cortices suggested by ECoG spectral amplitude analyses and visual symptoms induced by neurostimulation is described in Figures 2 and 3. In short, neurostimulation of the anterior-medial occipital cortex induced a phosphene in the contralateral peripheral field in six children, eye deviation toward the contralateral side in one child and no symptom in the remaining two children. Neurostimulation of the lateral-polar occipital cortex induced a phosphene in the central field in six children and no symptom in the remaining three children. Reported phosphenes were characterized by simple, bright, short-lasting flash with either dot, circular or unformed shape; none of the subjects reported a complex-form object associated with neurostimulation. A single child (patient #9) reported that the size of phosphene was larger when the anterior-medial occipital cortex was stimulated compared to when the lateral-polar occipital cortex was stimulated. The size of visual-related cortices suggested by significant gamma-augmentation on ECoG analyses was larger than that of neurostimulation. No other visual-related symptoms (such as formed visual hallucination) were induced by neurostimulation in the inferior occipital-temporal region or the posterior frontal region in the present study.

Four children (patients #2, 3, 5, and 9) had surgical resection involving both anterior-medial as well as the lateral-polar occipital cortices and developed a hemianopsia postoperatively (Table 1). A child (patient #6) who had a temporal lobectomy developed a quadrant hemianopsia postoperatively (Table 1). None of the remaining subjects postoperatively developed visual field deficits detected by confrontation tests.

## DISCUSSION

The major findings in the present study can be summarized in three points. i) Full-field stroboscopic flash stimuli induced gamma-augmentation in the anterior-medial occipital cortex (the anterior-medial surface of Brodmann Area 17/18) starting on average at 31 msec after stimulus presentation and subsequently in the lateral-polar occipital cortex (the lateral-to-polar surface of Brodmann Area 17/18), while minimal gamma oscillations were noted in the inferior occipital-temporal cortex (the inferior surface of Brodmann Area 19/37). ii) As best shown in animation movies (Video S2 and S4), central-field picture stimuli induced sustained gamma augmentation in the lateral-polar occipital cortex starting on average at 69 msec, subsequently in the inferior occipital-temporal cortex in all children, and in the posterior frontal cortex in three children; the anterior-medial occipital cortex showed no gamma augmentation but rather brief gamma attenuation. iii) Electrical stimulation of the anterior-medial occipital cortex induced a phosphene in the contralateral peripheral field, whereas that of the lateral-polar occipital cortex induced a phosphene in the more central field. These results increase our understanding of the physiology of the human visual system.

### Significance of gamma augmentation and attenuation in the anterior-medial occipital cortex following flash visual stimulus

The present study using intracranial ECoG recording demonstrated that the initial cortical activation represented as gamma augmentation occurred on average at 31 msec following short-lasting full-field flash stimuli in humans. This novel observation is quite consistent with a previous study of four macaque monkeys using intracranial unit recording showing that most units in the striate cortex had visual response latencies in the range of 30–50 msec under the stimulus conditions used and that the shortest latency recorded in the four animals ranged from 20 to 31 msec (Maunsell and Gibson, 1992). A recent study of six healthy adults using MEG also showed that the initial peak of visual-evoked magnetic fields following full-field flash stimuli was about 37 msec; a single equivalent current dipole analysis estimated the generator of this peak located in a part of the medial occipital striate cortex (Inui et al., 2006). A previous study of adults with focal epilepsy using intracranial ECoG recording demonstrated that checkerboard pattern stimuli presented in the central field yielded a visually-evoked response in the occipital pole initially exceeding the baseline voltage level at 56 msec (Yoshor et al., 2007).

The present study also demonstrated how the neural processing for full-field flash stimulus involved the areas surrounding the striate cortex. As best seen on an animation movie (Video S1) in the present study, flash visual stimulation induced augmentation of gamma oscillations initially in the anterior-medial occipital cortex, subsequently in the lateral-polar occipital cortex, while minimal gamma augmentation was noted in the inferior occipital-temporal cortex known as a part of visual association cortex (Kaas and Lyon, 2001). Preferential activation of the anterior-medial occipital cortex may be associated with full-field, short-lasting visual stimulus used in the present study. Since full-field flash visual stimulus was given with the eyes closed in a darkened room, we speculate that visual stimulus was processed initially by the retinal rod-photoreceptors sensitive to scattered light, concentrated in the periphery of the retina, and outnumbering the cone-photoreceptors (Kandel et al., 2000). Visual signals processed by the periphery of the retina are known to be transmitted to the anterior-medial striate cortex, according to previous studies of adults with occipital lesions using anatomical MRI and healthy adults using functional MRI (Wond and Sharpe, 1999; Levy et al., 2001;Stenbacka and Vanni, 2007). Previous studies of adults with focal epilepsy (Yoshor et al., 2007) and anesthetized monkeys (Rols et al, 2001) using intracranial ECoG recording showed that visual stimuli presented in the peripheral field yielded a visually-evoked potential (Yoshor et al., 2007) and gamma augmentation (Rols et al, 2001) predominantly involving the

medial occipital region and those in the central field yielded such cortical responses predominantly involving the lateral occipital region. In the present study, furthermore, neurostimulation confirmed that the anterior-medial occipital cortex showing the flash stimuli-induced gamma augmentation was a part of the primary visual cortex for the peripheral field in a substantial proportion of subjects.

The present study also provided a novel observation that full-field flash stimulus induced occipital gamma augmentation followed by significant gamma attenuation in three out of the nine children. We speculate that such brief gamma attenuation may represent a relative refractory period following the neural processing of flash stimulus, and refractoriness may occur between the retinal and cortical levels. A previous study of healthy adults using functional MRI showed that checkerboard pattern stimuli with an in interpair interval of 1 sec induced a hemodynamic response from the visual cortex 45% less than that with an interpair interval of 6 sec (Huettel and McCarthy, 2000). A study of ganglion cells in the isolated retina of the larval tiger salamanders using multi-microelectrode arrays showed that the firing rate from ganglion cells was decreased following each flicker visual stimulus (Berry and Meister, 1998). On the other hand, a study of healthy adults using transcranial magnetic stimulation revealed that a paired-pulse occipital stimulation with an inter-stimulus interval of 67 msec rather reduced the phosphene threshold to 74% of the threshold for single pulses (Gothe et al., 2002). Another possible explanation for the observation of occipital gamma attenuation following flash-induced gamma augmentation includes feed-forward inhibition by other areas (Shapley et al., 2003; Blitz and Regehr, 2005; Mariño et al., 2005; Priebe and Ferster, 2008).

### Significance of successive gamma augmentation involving the lateral-polar occipital, inferior occipital-temporal and posterior frontal cortices

The present study demonstrated that central-field picture stimuli induced successive gamma augmentation involving the lateral-polar occipital cortex (the primary visual cortex for the central field) and the inferior occipital-temporal cortex regardless of recorded hemisphere; the anterior-medial occipital cortex (the primary visual cortex for the peripheral field) showed no gamma augmentation but rather gamma attenuation during stimulus presentation in some children. These observations add complementary data to the previous human studies of visually-induced gamma modulation using intracranial depth electrodes (Lachaux et al., 2005; Tallon-Baudry et al., 2005). These studies clearly demonstrated sustained gamma augmentation in the lateral occipital cortex and the inferior occipital-temporal area, both of which were considered to play a role in visual object processing (Lachaux et al., 2005; Tallon-Baudry et al., 2005). Yet, these studies did not fully explain the observation of gamma attenuation in the anterior-medial striate cortex during central-field picture stimulus (Lachaux et al., 2005), possibly because of the lack of sampling from the primary visual cortex for the central field (Tallon-Baudry et al., 2005). In the present study, ECoG assessment revealed gamma attenuation in the primary visual cortex for the peripheral field, while gamma oscillations in the primary visual cortex for the central field were augmented. Thus, we speculate that gamma attenuation in the anterior-medial occipital cortex during central-filed object visualization may be associated with relative inattention to the peripheral visual field during presentation of central-field picture stimuli.

The present study demonstrated a novel observation that gamma augmentation was noted in the posterior frontal area following central-field picture stimuli in three children (Table 3; Video S4). One of the plausible interpretations of this posterior frontal gamma augmentation during picture stimuli includes activation of frontal eye field for visual searching. As most children love watching TV, our subjects appeared to actively attend the visual tasks, although no other tasks (such as pressing button) were assigned in the present study. In order to increase attention of subjects, we selected a variety of pictures including faces, houses and abstract

shapes. A previous study of healthy adults using functional MRI revealed a hemodynamic activation in the bilateral frontal eye fields associated with central-field simple picture stimulus (Mukai et al., 2007). A previous study of healthy adults using high-density scalp EEG recording reported that the source of ERP peak associated with visual searching was estimated to be located in the frontal eye field (Saron et al., 2001). We currently plan to investigate the temporal and spatial patterns of gamma modulation in the frontal region, using the eye-tracking system, which would allow assessment of ECoG changes time-locked to the onset of eye movement (Yuval-Greenberg et al, 2008).

### Methodological limitations in the present study

Potential methodological limitations of our study should be discussed. One of the major limitations of extraoperative ECoG recordings is sampling error. In the present study, subdural electrodes were placed only in the presumed epileptogenic hemisphere; we were not able to evaluate cortical activation in the other hemisphere. Electrode placement was also limited by the location of bridging veins abundant in the posterior head region. Thus, neither lack of cortical activation on ECoG analysis nor lack of clinical symptoms induced by neurostimulation provides evidence for the absence of cortical function in the present study. Since the assumption that subdural electrodes covered the same anatomical locations across the subjects was not tenable in the present study, we were not able to determine the relationship between the age of subjects and the characteristics of visually-induced gamma augmentation.

Failure to induce a clinical symptom using neurostimulation of a cortical site does not prove the absence of eloquent function in that site in children. Previous studies of humans (Haseeb et al., 2007) and cats (Chakrabarty and Martin, 2000) showed that neurostimulation of the Rolandic cortex more frequently failed to elicit motor responses in younger subjects. Another human study using transcranial magnetic stimulation showed that the motor threshold was negatively correlated with the age of subjects (Muller et al., 1991). Previous studies of children with focal epilepsy showed that neurostimulation via subdural electrodes frequently failed to induce language symptoms in children younger than 10 years old (Ojemann et al., 2003; Schevon et al., 2007). It has been speculated that immature development of cortical myelination may be associated with failure to electrically induce clinical responses in young children (Muller et al., 1991).

The location of a phosphene induced by neurostimulation was determined not quantitatively but qualitatively in the present study. Thus, the present study failed to confirm fine estimates of the retinotropic organization of the occipital cortex. A previous study of adults with focal epilepsy using intracranial ECoG recording estimated the retinotropic organization of the occipital cortex using the amplitude of visual-evoked potentials (Yoshor et al., 2007). A future study using a similar experimental task may determine how visual stimuli at each visual field induce alteration of gamma-oscillations at each occipital site.

In the present study of children undergoing extraoperative ECoG recording, the protocol did not include a visual task consisting of purely-peripheral visual stimuli. Presentation of visual stimuli solely in the peripheral field has remained a challenge in human studies (Stenbacka and Vanni, 2007), since subjects are required to fixate a central point of the monitor while visual stimuli are presented peripherally. The majority of previous human studies to delineate peripheral visual field representation using functional MRI and intracranial ECoG were performed in adults not children.

Central-field picture stimuli had a larger amount of semantic information compared to full-field stroboscopic stimuli in the present study. Thus, these two visual stimulus conditions not only varied by the extent of the visual field covered, but also varied by the amount of semantic information. It is therefore possible that the differential cortical activation induced by two

different visual tasks may be at least partly explained by the difference in the amount of semantic information in the visual stimuli. Future studies using a different combination of visual tasks may determine what portion of cortical activation is explained by the amount of semantic information and what is explained by the topography of visual field.

Antiepileptic drugs may affect the findings of cortical mapping using neurostimulation as well as measurement of gamma-oscillations on ECoG. In the present study, phenytoin was loaded intravenously prior to the mapping session to minimize the risk of stimulation-induced seizures. A previous study of healthy adults demonstrated that phenytoin elevated motor thresholds to transcranial magnetic stimulation but had no effect on motor-evoked potential amplitudes, silent period duration, or intracortical excitability (Chen et al., 1997).

It has been reported that no truly ‘inactive’ reference is available in clinical EEG studies and any analytic approach using any reference has some limitations (Pivik et al., 1993). In the present study, ECoG amplitude measures were calculated using a common average reference. Usage of a common average reference has been previously reported in previous ECoG studies in which event-related gamma-oscillations were measured (Crone et al., 2001; Tanji et al., 2005; Fukuda et al., 2008; Brown et al., 2008; Towle et al., 2008). Yet, the common average reference unavoidably introduces a common signal into all channels; the unwanted influence of such a common signal may alter ECoG amplitude measures, when only a small number of intracranial electrodes are implanted or when even a large number of electrodes were placed on a restricted area of interest. In a previous study of event-related gamma-oscillations, where only five to nine electrodes were included into time-frequency analysis, not a common average reference but a most inactive electrode overlying the brain tumor was selected as a reference electrode (Edwards et al., 2005). In another study where a single grid electrode array (containing 27 – 36 electrodes) was placed in the posterior temporal region of interest (Tallon-Baudry et al., 2004), a current source density approach based on splines (Perrin et al., 1987) was applied in order to suppress the effect of the common reference. On the other hand, a previous study using scalp EEG recording suggested that the common average reference derived from a large number of electrodes (such as 128 channels) can provide a good approximation of an inactive reference (Junghöfer et al., 1999). In the present study, the total number of intracranial electrodes ranged from 96 to 128 (per subject); combination of grid and strip electrodes were placed on widespread regions involving all four cerebral lobes. None of the subjects showed significant gamma-augmentation or gamma-attenuation simultaneously involving all electrode sites; differential visually-induced gamma augmentation involving two occipital regions was consistent with cortical stimulation findings. Thus, we speculate that the effect of signal distortion derived from a common average reference on ECoG amplitude measures was small in the present study.

## Supplementary Material

Refer to Web version on PubMed Central for supplementary material.

## Acknowledgments

This work was supported by NIH grant NS47550 (to E. A.). We are grateful to Harry T Chugani, M.D., Carol Pawlak, R.EEG/EP.T, Ruth Roeder, R.N., M.S. and the staff of the Division of Electroneuro diagnostics at Children’s Hospital of Michigan, Wayne State University for the collaboration and assistance in performing the studies described above.

## References

Auranen, T. Nonparametric statistical analysis of time-frequency representations of magnetoencephalographic data. Master’s Thesis, Helsinki University of Technology, Department of Electrical and Communications Engineering; Espoo, Finland. 2002.

Berry MJ 2nd, Meister M. Refractoriness and neural precision. J Neurosci 1998;18:2200–2211. [PubMed: 9482804]

Blitz DM, Regehr WG. Timing and specificity of feed-forward inhibition within the LGN. Neuron 2005;45:917–928. [PubMed: 15797552]

Brown EC, Rothermel R, Nishida M, Juhász C, Muzik O, Hoechstetter K, Sood S, Chugani HT, Asano E. In-vivo animation of auditory-language-induced gamma-oscillations in children with intractable focal epilepsy. Neuroimage 2008;41:1120–1131. [PubMed: 18455440]

Bruns A, Eckhorn R. Task-related coupling from high- to low-frequency signals among visual cortical areas in human subdural recordings. Int J Psychophysiol 2004;51:97–116. [PubMed: 14693360]

Chakrabarty S, Martin JH. Postnatal development of the motor representation in primary motor cortex. J Neurophysiol 2004;84:2582–2594. [PubMed: 11068000]

Chen R, Samii A, Canos M, Wassermann EM, Hallett M. Effects of phenytoin on cortical excitability in humans. Neurology 1997;49:881–883. [PubMed: 9305361]

Coburn KL, Amoss RT, Arruda JE, Kizer LD, Marshall YS. Effects of flash mode and intensity on P2 component latency and amplitude. Int J Psychophysiol 2005;55:323–331. [PubMed: 15708645]

Crone NE, Miglioretti DL, Gordon B, Lesser RP. Functional mapping of human sensorimotor cortex with electrocorticographic spectral analysis. II Event-related synchronization in the gamma band Brain 1998;121:2301–2315.

Crone NE, Boatman D, Gordon B, Hao L. Induced electrocorticographic gamma activity during auditory perception. Brazier Award-winning article Clin Neurophysiol 2001;112:565–582.

Csibra G, Davis G, Spratling MW, Johnson MH. Gamma oscillations and object processing in the infant brain. Science 2000;290:1582–1585. [PubMed: 11090357]

da Silva, FL. EEG analysis: theory and practice. In: Niedermeyer, E.; da Silva, FL., editors. Electroencephalography. Vol. 4. Williams and Wilkins; Baltimore: 1999. p. 1135-1163.

Davidson, AC.; Hinkley, DV. Bootstrap Methods and their Application, Chapter 4.4.1: Studentized bootstrap method. Cambridge University Press; Cambridge: 1999. p. 161-175.

Di Russo F, Pitzalis S, Aprile T, Spitoni G, Patria F, Stella A, Spinelli D, Hillyard SA. Spatiotemporal analysis of the cortical sources of the steady-state visual evoked potential. Hum Brain Mapp 2007;28:323–334. [PubMed: 16779799]

Edwards E, Soltani M, Deouell LY, Berger MS, Knight RT. High gamma activity in response to deviant auditory stimuli recorded directly from human cortex. J Neurophysiol 2005;94:4269–4280. [PubMed: 16093343]

Fan J, Byrne J, Worden MS, Guise KG, McCandliss BD, Fossella J, Posner MI. The relation of brain oscillations to attentional networks. J Neurosci 2007;27:6197–6206. [PubMed: 17553991]

Farrell DF, Leeman S, Ojemann GA. Study of the human visual cortex: direct cortical evoked potentials and stimulation. J Clin Neurophysiol 2007;24:1–10. [PubMed: 17277570]

Fukuda M, Nishida M, Juhasz C, Muzik O, Sood S, Chugani HT, Asano E. Short-latency median-nerve somatosensory-evoked potentials and induced gamma-oscillations in humans. Brain 2008;131:1793–1805. [PubMed: 18508784]

Gaillard R, Naccache L, Pinel P, Clemenceau S, Volle E, Hasboun D, Dupont S, Baulac M, Dehaene S, Adam C, Cohen L. Direct intracranial, FMRI, and lesion evidence for the causal role of left inferotemporal cortex in reading. Neuron 2006;50:191–204. [PubMed: 16630832]

Gothe J, Brandt SA, Irlbacher K, Röricht S, Sabel BA, Meyer BU. Changes in visual cortex excitability in blind subjects as demonstrated by transcranial magnetic stimulation. Brain 2002;125:479–490. [PubMed: 11872606]

Gray CM, McCormick DA. Chattering cells: superficial pyramidal neurons contributing to the generation of synchronous oscillations in the visual cortex. Science 1996;274:109–113. [PubMed: 8810245]

Hoechstetter K, Bornfleth H, Weckesser D, Ille N, Berg P, Scherg M. BESA source coherence: A new method to study cortical oscillatory coupling. Brain Topography 2004;16:233–238. [PubMed: 15379219]

Holmes G, Lister WT. Disturbances of vision from cerebral lesion with special reference to the cortical representation of the macula. Brain 1916;39:34–73.

Huettel SA, McCarthy G. Evidence for a refractory period in the hemodynamic response to visual stimuli as measured by MRI. Neuroimage 2000;11:547–553. [PubMed: 10806040]

Huettel SA, McKeown MJ, Song AW, Hart S, Spencer DD, Allison T, McCarthy G. Linking hemodynamic and electrophysiological measures of brain activity: evidence from functional MRI and intracranial field potentials. Cereb Cortex 2004;14:165–173. [PubMed: 14704213]

Inui K, Sannan H, Miki K, Kaneoke Y, Kakigi R. Timing of early activity in the visual cortex as revealed by simultaneous MEG and ERG recordings. Neuroimage 2006;30:239–244. [PubMed: 16310379]

Junghöfer M, Elbert T, Tucker DM, Braun C. The polar average reference effect: a bias in estimating the head surface integral in EEG recording. Clin Neurophysiol 1999;110:1149–1155. [PubMed: 10402104]

Kaa JH, Lyon DC. Visual cortex organization in primates: theories of V3 and adjoining visual areas. Prog Brain Res 2001;134:285–295. [PubMed: 11702549]

Kandel, ER.; Schwartz, JH.; Jessell, TM. Principles of Neural Science. Vol. 4. New York: McGraw-Hill; 2000. p. 507-513.

Klem, GH. Artifacts. In: Ebersole, JS.; Pedley, TA., editors. Current practice of clinical electroencephalography. Lippincott Williams and Wilkins; Philadelphia: 2003. p. 271-287.

Kruse W, Eckhorn R. Inhibition of sustained gamma oscillations (35–80 Hz) by fast transient responses in cat visual cortex. Proc Natl Acad Sci USA 1996;93:6112–6117. [PubMed: 8650228]

Lachaux JP, George N, Tallon-Baudry C, Martinerie J, Hugueville L, Minotti L, Kahane P, Renault B. The many faces of the gamma band response to complex visual stimuli. Neuroimage 2005;25:491–501. [PubMed: 15784428]

Levy I, Hasson U, Avidan G, Hendler T, Malach R. Center-periphery organization of human object areas. Nat Neurosci 2001;4:533–539. [PubMed: 11319563]

Mariño J, Schummers J, Lyon DC, Schwabe L, Beck O, Wiesing P, Obermayer K, Sur M. Invariant computations in local cortical networks with balanced excitation and inhibition. Nat Neurosci 2005;8:194–201. [PubMed: 15665876]

Maunsell JH, Gibson JR. Visual response latencies in striate cortex of the macaque monkey. J Neurophysiol 1992;68:1332–1344. [PubMed: 1432087]

Miller KJ, Leuthardt EC, Schalk G, Rao RP, Anderson NR, Moran DW, Miller JW, Ojemann JG. Spectral changes in cortical surface potentials during motor movement. J Neurosci 2007;27:2424–2432. [PubMed: 17329441]

Müller K, Hömberg V, Lenard HG. Magnetic stimulation of motor cortex and nerve roots in children. Maturation of cortico-motoneuronal projections Electroencephalogr Clin Neurophysiol 1991;81:63–70.

Mukai I, Kim D, Fukunaga M, Japee S, Marrett S, Ungerleider LG. Activations in visual and attention-related areas predict and correlate with the degree of perceptual learning. J Neurosci 2007;27:11401–11411. [PubMed: 17942734]

Muzik O, Chugani DC, Zou G, Hua J, Lu Y, Lu S, Asano E, Chugani HT. Multimodality Data Integration in Epilepsy. Int J Biomed Imaging. 200710.1155/2007/13963

Niessing J, Ebisch B, Schmidt KE, Niessing M, Singer W, Galuske RA. Hemodynamic signals correlate tightly with synchronized gamma oscillations. Science 2005;309:948–951. [PubMed: 16081740]

Nishida M, Asano E, Juhász C, Muzik O, Sood S, Chugani HT. Cortical glucose metabolism correlates negatively with delta slowing wave and spike frequency in epilepsy associated with tuberous sclerosis. Hum Brain Mapp. 200710.1002/hbm.20461

Nobre AC, Sebestyen GN, Gitelman DR, Mesulam MM, Frackowiak RS, Frith CD. Functional localization of the system for visuospatial attention using positron emission tomography. Brain 1997;120:515–533. [PubMed: 9126062]

Ohla K, Busch NA, Herrmann CS. Early electrophysiological markers of visual awareness in the human brain. Neuroimage 2007;37:1329–1337. [PubMed: 17656113]

Ojemann SG, Berger MS, Lettich E, Ojemann GA. Localization of language function in children: results of electrical stimulation mapping. J Neurosurg 2003;98:465–470. [PubMed: 12650415]

Papp N, Ktonas P. Critical evaluation of complex demodulation techniques for the quantification of bioelectrical activity. Biomed Sci Instrum 1977;13:135–145. [PubMed: 871500]

Pavlova M, Lutzenberger W, Sokolov A, Birbaumer N. Dissociable cortical processing of recognizable and non-recognizable biological movement: analysing gamma MEG activity. Cereb Cortex 2004;14:181–188. [PubMed: 14704215]

Perrin F, Bertrand O, Pernier J. Scalp current density mapping: value and estimation from potential data. IEEE Trans Biomed Eng 1987;34:283–188. [PubMed: 3504202]

Pfurtscheller G. Graphical display and statistical evaluation of event-related desynchronization (ERD). Electroencephalogr Clin Neurophysiol 1977;43:757–760. [PubMed: 72657]

Pivik RT, Broughton RJ, Coppola R, Davidson RJ, Fox N, Nuwer MR. Guidelines for the recording and quantitative analysis of electroencephalographic activity in research contexts. Psychophysiology 1993;30:547–558. [PubMed: 8248447]

Poghosyan V, Ioannides AA. Precise mapping of early visual responses in space and time. Neuroimage 2007;35:759–770. [PubMed: 17275339]

Priebe NJ, Ferster D. Inhibition, spike threshold, and stimulus selectivity in primary visual cortex. Neuron 2008;57:482–497. [PubMed: 18304479]

Prado J, Clavagnier S, Otzenberger H, Scheiber C, Kennedy H, Perenin MT. Two cortical systems for reaching in central and peripheral vision. Neuron 2005;48:849–858. [PubMed: 16337921]

Privman E, Nir Y, Kramer U, Kipervasser S, Andelman F, Neufeld MY, Mukamel R, Yeshurun Y, Fried I, Malach R. Enhanced category tuning revealed by intracranial electroencephalograms in high-order human visual areas. J Neurosci 2007;27:6234–6242. [PubMed: 17553996]

Rols G, Tallon-Baudry C, Girard P, Bertrand O, Bullier J. Cortical mapping of gamma oscillations in areas V1 and V4 of the macaque monkey. Vis Neurosci 2001;18:527–540. [PubMed: 11829299]

Rudrauf D, David O, Lachaux JP, Kovach CK, Martinerie J, Renault B, Damasio A. Rapid interactions between the ventral visual stream and emotion-related structures rely on a two-pathway architecture. J Neurosci 2008;28:2793–2803. [PubMed: 18337409]

Salmelin R, Hari R. Spatiotemporal characteristics of sensorimotor MEG rhythms related to thumb movement. Neuroscience 1994;60:537–550. [PubMed: 8072694]

Saron CD, Schroeder CE, Foxe JJ, Vaughan HG Jr. Visual activation of frontal cortex: segregation from occipital activity. Brain Res Cogn Brain Res 2001;12:75–88. [PubMed: 11489611]

Schevon CA, Carlson C, Zaroff CM, Weiner HJ, Doyle WK, Miles D, Lajoie J, Kuzniecky R, Pacia S, Vazquez B, Luciano D, Najjar S, Devinsky O. Pediatric language mapping: sensitivity of neurostimulation and Wada testing in epilepsy surgery. Epilepsia 2007;48:539–545. [PubMed: 17284300]

Sederberg PB, Schulze-Bonhage A, Madsen JR, Bromfield EB, Litt B, Brandt A, Kahana MJ. Gamma oscillations distinguish true from false memories. Psychol Sci 2007;18:927–932. [PubMed: 17958703]

Shapley R, Hawken M, Ringach DL. Dynamics of orientation selectivity in the primary visual cortex and the importance of cortical inhibition. Neuron 2003;38:689–699. [PubMed: 12797955]

Simes RJ. An improved Bonferroni procedure for multiple tests of significance. Biometrika 1986;73:751–754.

Sinai A, Bowers CW, Crainiceanu CM, Boatman D, Gordon B, Lesser RP, Lenz FA, Crone NE. Electrocorticographic high gamma activity versus electrical cortical stimulation mapping of naming. Brain 2005;128:1556–1570. [PubMed: 15817517]

Stenbacka L, Vanni S. fMRI of peripheral visual field representation. Clin Neurophysiol 2007;118:1303–1314. [PubMed: 17449320]

Talairach, J.; Tournoux, P. Co-planar stereotaxic atlas of the human brain. New York: Thieme; 1988.

Tallon-Baudry C, Bertrand O, Delpuech C, Pernier J. Stimulus specificity of phase-locked and non-phase-locked 40 Hz visual responses in human. J Neurosci 1996;16:4240–4249. [PubMed: 8753885]

Tallon-BaudryCBertrand O, Fischer C. Oscillatory synchrony between human extrastriate areas during visual short-term memory maintenance. J Neurosci 2001;21:RC177. [PubMed: 11588207]

Tallon-Baudry C, Mandon S, Freiwald WA, Kreiter AK. Oscillatory synchrony in the monkey temporal lobe correlates with performance in a visual short-term memory task. Cereb Cortex 2004;14:713–720. [PubMed: 15054050]

Tallon-Baudry C, Bertrand O, Hénaff MA, Isnard J, Fischer C. Attention modulates gamma-band oscillations differently in the human lateral occipital cortex and fusiform gyrus. Cereb Cortex 2005;15:654–662. [PubMed: 15371290]

Tanji K, Suzuki K, Delorme A, Shamoto H, Nakasato N. High-frequency gamma-band activity in the basal temporal cortex during picture-naming and lexical-decision tasks. J Neurosci 2005;25:3287–3293. [PubMed: 15800183]

Towle VL, Yoon HA, Castelle M, Edgar JC, Biassou NM, Frim DM, Spire JP, Kohrman MH. ECoG gamma activity during a language task: differentiating expressive and receptive speech areas. Brain 2008;131:2013–2027. [PubMed: 18669510]

Vandenberghe R, Duncan J, Arnell KM, Bishop SJ, Herrod NJ, Owen AM, Minhas PS, Dupont P, Pickard JD, Orban GA. Maintaining and shifting attention within left or right hemifield. Cereb Cortex 2000;10:706–713. [PubMed: 10906317]

Vingerhoets RA, Van Gisbergen JA, Medendorp WP. Verticality perception during off-vertical axis rotation. J Neurophysiol 2007;97:3256–3268. [PubMed: 17329621]

von Stockhausen HM, Thiel A, Herholz K, Pietrzyk U. A convenient method for topographical localization of intracranial electrodes with MRI and a conventional radiograph. Neuroimage 1997;5:S514.

Wang Y, Gotman J. The influence of electrode location errors on EEG dipole source localization with a realistic head model. Clin Neurophysiol 2001;112:1777–1780. [PubMed: 11514261]

Womelsdorf T, Fries P, Mitra PP, Desimone R. Gamma-band synchronization in visual cortex predicts speed of change detection. Nature 2006;439:733–736. [PubMed: 16372022]

Wong AM, Sharpe JA. Representation of the visual field in the human occipital cortex: a magnetic resonance imaging and perimetric correlation. Arch Ophthalmol 1999;117:208–217. [PubMed: 10037566]

Woods, DL.; Yund, EW.; Kang, XJ. Unified functional/anatomical maps of human auditory cortex. Archives of Neurobehavioral Experiments and Stimuli 46. 2004. (Link to http://www.neurobs.com/ex_files/expt_view?id=46)

Yoshor D, Bosking WH, Ghose GM, Maunsell JH. Receptive fields in human visual cortex mapped with surface electrodes. Cereb Cortex 2007;17:2293–2302. [PubMed: 17172632]

Yotsumoto Y, Watanabe T, Sasaki Y. Different dynamics of performance and brain activation in the time course of perceptual learning. Neuron 2008;57:827–833. [PubMed: 18367084]

Yuval-Greenberg S, Tomer O, Keren AS, Nelken I, Deouell LY. Transient induced gamma-band response in EEG as a manifestation of miniature saccades. Neuron 2008;58:429–441. [PubMed: 18466752]

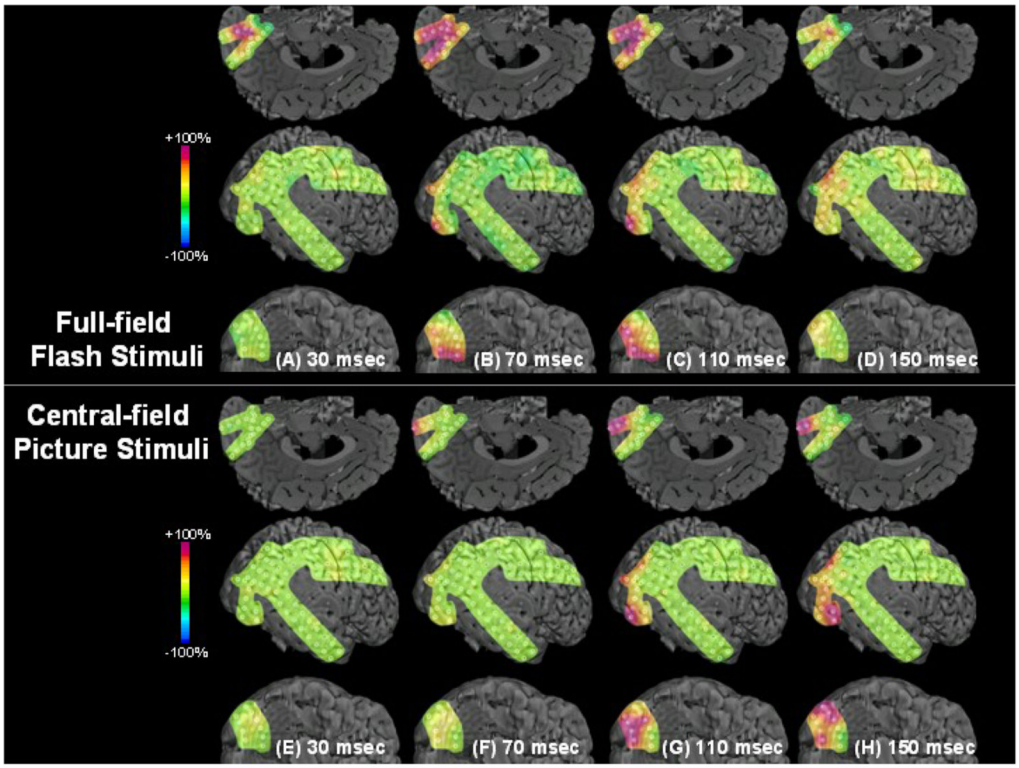


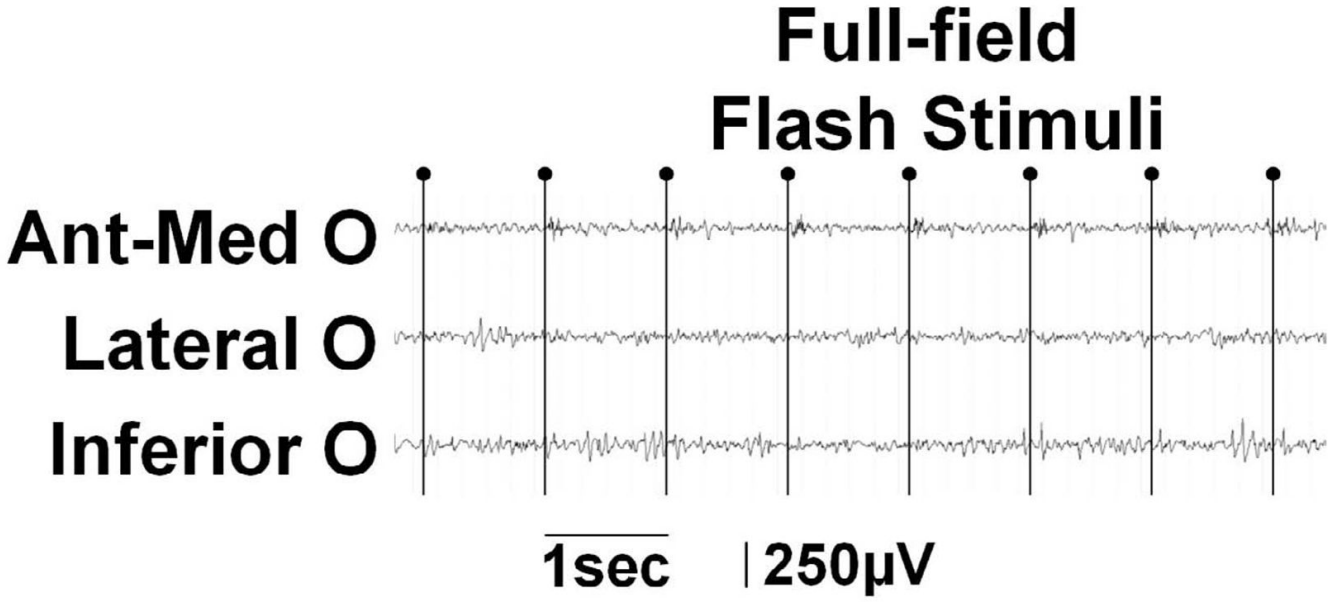

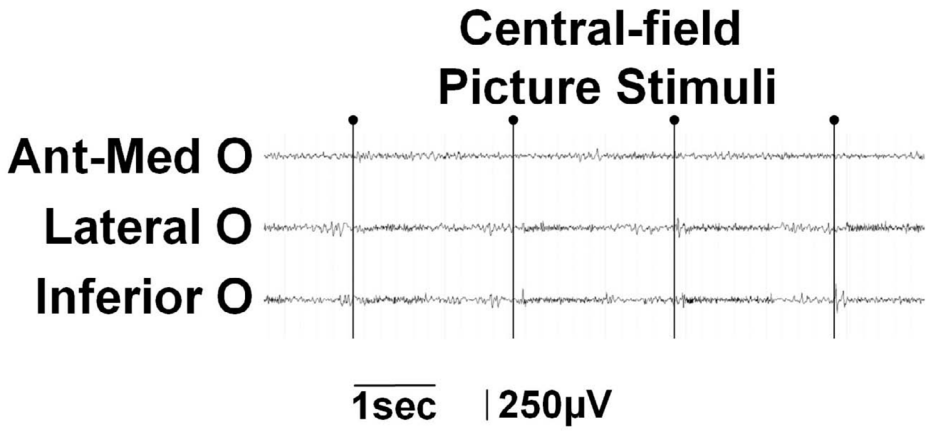


**Figure 1. Results of visual mapping using ECoG amplitude analysis and neurostimulation in a 17-year-old girl with uncontrolled focal epilepsy (Patient #9)**

(A–D) Full-field flash stimuli (upper frames) induced short-lasting gamma augmentation (red) initially involving the right anterior-medial occipital area and subsequently in the lateral-polar occipital area. Minimal gamma-augmentation was noted in the inferior occipital-temporal area. (E–H) Central-field picture stimuli (lower frames) induced sustained gamma augmentation initially involving the lateral-polar occipital area and subsequently involving the inferior occipital-temporal area; no gamma-augmentation was noted in the anterior-medial occipital area. (I) ECoG traces during full-field flash stimuli are presented. Brief gamma augmentation was noted in the anterior-medial occipital area following each flash stimulus. Oval arrows indicate the onset of stimuli. Low-frequency filter: 53 Hz. High-frequency filter: 300 Hz. (J) ECoG traces during central-field picture stimuli are presented. Sustained gamma augmentation was noted in the lateral and inferior occipital areas during presentation of stimuli.

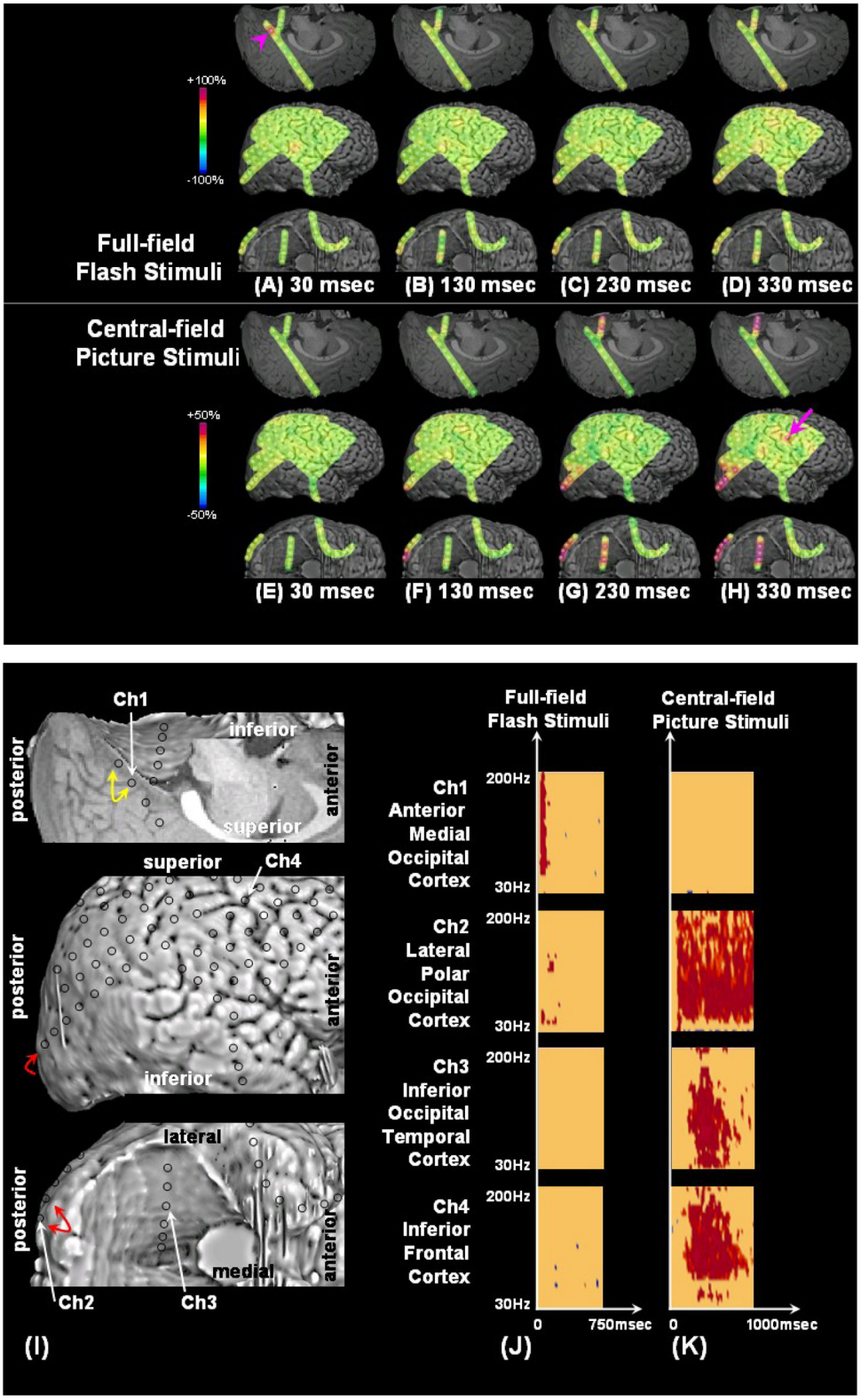


**Figure 2. Results of visual mapping using ECoG amplitude analysis and neurostimulation in a 7-year-old boy with uncontrolled focal epilepsy (Patient #4)**

(A–D) Full-field flash stimuli (upper frames) induced short-lasting gamma augmentation (red) involving the right anterior-medial occipital area (arrowhead). (E–H) Central picture stimuli (lower frames) induced sustained gamma augmentation initially involving the lateral-polar occipital area and subsequently involving the inferior occipital-temporal area. Sustained gamma augmentation was also noted in the right frontal region just front of the precentral gyrus (arrow). (I) Neurostimulation of the anterior-medial occipital region (yellow arrow) induced a white circular phosphene in the left-side peripheral field, whereas neurostimulation of the occipital polar region (red arrow) induced a white circular phosphene in the more central field. (J) Time-frequency plot matrixes show that full-field flash stimuli induced significant gamma augmentation initially in the anterior-medial occipital cortex and subsequently in the lateral-polar occipital cortex. (K) Central-field picture stimuli induced significant gamma augmentation initially in the lateral-polar occipital cortex and subsequently in the inferior occipital-temporal area. Sustained gamma augmentation was also noted in the right frontal region just front of the precentral gyrus.

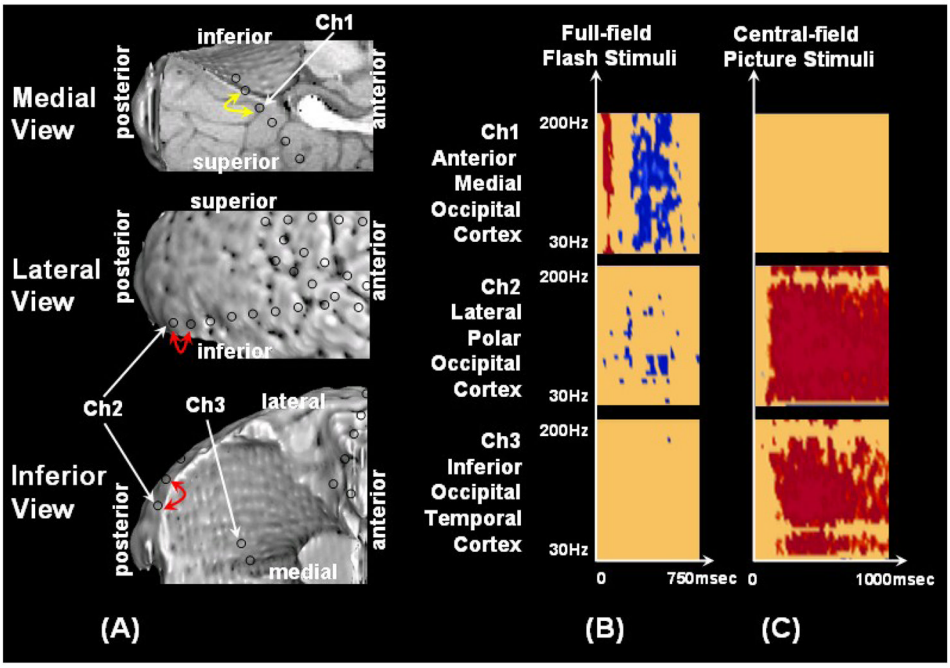


**Figure 3. Results of visual mapping using ECoG amplitude analysis and neurostimulation in a 5-year-old girl with uncontrolled focal epilepsy (Patient #3)**

(A) Neurostimulation of the anterior-medial occipital region (yellow arrow) induced a phosphene in the left-side peripheral field, whereas neurostimulation of the occipital polar region (red arrow) induced a phosphene in the more central field. The patient reported that she saw something bright but could not describe the exact shape or color. (B) Full-field flash stimuli resulted in short-lasting gamma augmentation (red) involving the right anterior-medial occipital area and subsequently resulted in gamma attenuation (blue) in the same area as well as the lateral-polar occipital area. (C) Central picture stimuli induced sustained gamma augmentation initially involving the lateral-polar occipital area and subsequently involving the inferior occipital-temporal area.

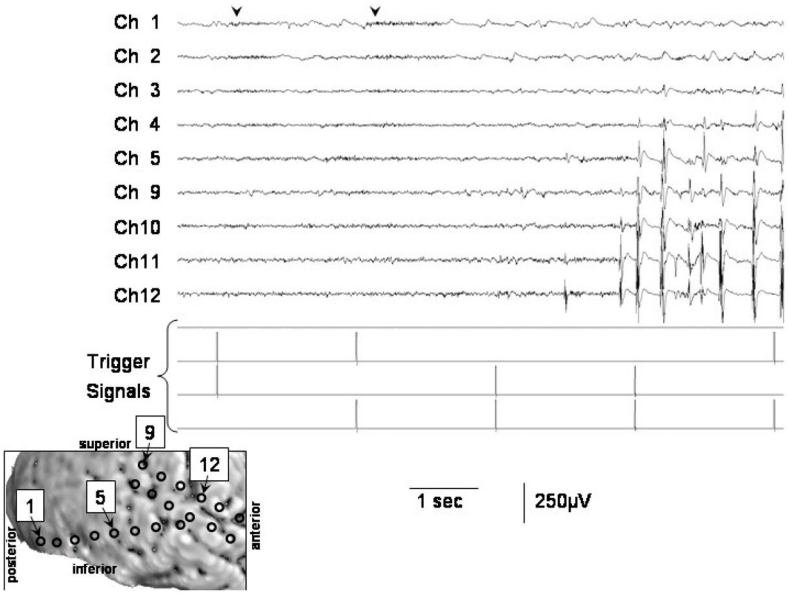


**Figure 4. ECoG trace during central-field picture stimuli in a 5-year-old girl with uncontrolled focal epilepsy (Patient #3)**

The first and second picture stimuli induced sustained gamma-augmentation (arrowheads) in Channels 1 and 2 on the right lateral occipital cortex. No such gamma-augmentation was noted following the third, fourth or fifth picture stimuli, when interictal spike-wave bursts involved the occipital cortex. Low-frequency filter: 50 Hz. High-frequency filter: 300 Hz. A repeat session of central-field picture presentation was employed to this subject in the following day and the results are shown in Figure 3.

**Table 1**

**Summary of Clinical Information**

Patients #2 and 5 were left-handed, whereas the remaining seven patients were right-handed. F: Female. M: Male. Lt: Left. Rt: Right. LEV: Levetiracetam. LGT: Lamotrigine. PHT: Phenytoin. OXC: Oxcarbazepine. TPM: Topiramate. VPA: Valproic acid. ZNS: Zonisamide. sGTC: Secondarily Generalized Tonic Clonic Seizures. F: Frontal. T: Temporal. O: Occipital. P: Parietal. C: Central. SBS: Secondary bilateral synchrony. CSWS: Continuous spike-wave discharges during slow-wave sleep. HS: Hippocampal sclerosis. VIQ: Verbal IQ. VCI: Verbal Comprehension Index. PIQ: Performance IQ. PRI: Perceptual Reasoning Index. POI: Perceptual Organization Index. FSIQ: Full Scale IQ.

| Patients | Gender | Age (yr) | Antiepileptic mediations | Seizure semiology | Interictal spikes on scalp EEG | Ictal EEG onset on scalp EEG | Electrode placement | Seizure onset zones determined on ECoG | Histology | VIQ/VCI | PIQ/PRI/POI | FSIQ |
|---|---|---|---|---|---|---|---|---|---|---|---|---|
| 1 | F | 3 | PHT | Focal, sGTC | Rt T | Not captured | Rt TOPF | Not captured but frequent interictal spikes were noted in Rt T | HS and Gliosis in the temporal neocortex | 71 | 60 | 60 |
| 2 | F | 4 | ZNS | Focal, Spasms | Lt CFPT | Lt CT | Lt TOPF | Lt TOPF | Dysplasia and Gliosis | 70 | 65 | 63 |
| 3 | F | 5 | TPM | Focal, sGTC | Rt POTF | Not captured but CSWS was noted | Rt POTF | Not captured but CSWS involving Rt POT was noted | Dysplasia | 98 | 81 | 87 |
| 4 | M | 7 | OXC, LEV, VPA | Focal, Spasms, sGTC | Rt CPFT | Rt CPF | Rt FPOT | Rt FP | Dysplasia | 85 | 108 | 109 |
| 5 | F | 7 | OXC, ZNS | Focal, sGTC | Lt POTC with SBS | Lt POT | Lt POTF | Lt T; Lt F | Gliosis | 75 | 84 | 75 |
| 6 | M | 14 | ZNS, LGT, TPM | Focal, sGTC | Rt T; Rt TP | Rt T | Rt TOPF | Rt T | HS and Gliosis in the temporal neocortex | 55 | 57 | 48 |
| 7 | M | 14 | OXC, TPM, LEV | Focal, Spasms, sGTC | Rt CPT | Rt CPT | Rt PFOT | Rt PT | Dysplasia | 77 | 82 | 64 |
| 8 | M | 15 | OXC | Focal, sGTC | Not captured | Not captured | Lt TOPF | Not captured but frequent interictal spikes were noted in Lt T | Tumor | 95 | 84 | 86 |
| 9 | F | 17 | OXC, LEV | Focal, sGTC | Rt OPT with SBS; Generalized | Rt OPT | Rt OPTF | Rt O | Gliosis | 100 | 97 | 95 |

*Neuroimage*. Author manuscript; available in PMC 2010 April 1.

## Table 2

**Visually-Induced Gamma Modulation Associated with Full-field Flash Stimuli**

The periods (after stimulus presentation) showing significant regional gamma-augmentation are shown. Similarly, the periods showing significant regional gamma-attenuation are shown in parentheses. NS: No significant gamma alteration.

| Patients | Gamma oscillations in the anterior-medial occipital region | Gamma oscillations in the lateral-polar occipital region | Gamma oscillations in the inferior occipital-temporal region | Gamma oscillations in the posterior frontal region |
|---|---|---|---|---|
| 1 | 30–230 | NS | 310–400 | NS |
| 2 | 30–250 | 30–140 | NS | NS |
| 3 | 50–120(240–610) | NS (200–510) | NS | NS |
| 4 | 30–130 | 50–180 | 120–320 | NS |
| 5 | 30–100 (210–480) | 50–190 (330–570) | NS | NS |
| 6 | 30–100 | 30–160 | 70–290 | NS |
| 7 | 30–330 (120–320) | 50–80 (420–630) | NS | NS |
| 8 | 30–180 | 50–130 | 260–390 | NS |
| 9 | 20–150 | 50–240 | 60–80 | NS |

## Table 3

**Visually-Induced Gamma Modulation Associated with Central-field Picture Stimuli**

The periods (after stimulus presentation) showing significant regional gamma-augmentation are shown. Similarly, the periods showing significant regional gamma-attenuation are shown in parentheses. NS: No significant gamma alteration.

| Patients | Gamma oscillations in the anterior-medial occipital region | Gamma oscillations in the lateral-polar occipital region | Gamma oscillations in the inferior occipital-temporal region | Gamma oscillations in the posterior frontal region |
|---|---|---|---|---|
| 1 | NS (320–640) | 120–930 | 210–1190 | 270–800 |
| 2 | NS | 50–1230 | 80–1370 | NS |
| 3 | NS | 80–1320 | 120–1150 | NS |
| 4 | NS | 70–1230 | 150–1240 | 150–880 |
| 5 | NS | 70–1180 | 210–800 | NS |
| 6 | NS | 60–1220 | 150–730 | NS |
| 7 | NS | 60–1260 | 100–700 | NS |
| 8 | NS (150–290) | 60–1250 | 100–1050 | 520–650 |
| 9 | NS (520–810) | 50–1230 | 70–1220 | NS |